

CONFIDENTIAL - UNCLASSIFIED - 144

LA-UR-79-15264

TITLE: A MULTIDIMENSIONAL ELECTROMETER DATA ACQUISITION SYSTEM

AUTHOR(S): Judith Sommers, Kenneth R. Hoggstrom, Roy T. Stilicee,
Isaac L. Rosenzweig, and Alfred R. Semitoff

SUBMITTED TO: Proceedings of the IEEE Nuclear Science Symposium
Santa Fe, NM May 14-17, 1979

MASTER

By accepting this manuscript, the publisher recognizes that the USG Government retains ownership, royalty free, to cause to publish or reproduce the publication formed by this manuscript, or to allow others to do so, for USG Government purposes.

This Los Alamos document was prepared under contract with the USG. It is subject to disclosure under the USG Freedom of Information Act.

University of California



LOS ALAMOS SCIENTIFIC LABORATORY

Post Office Box 1663 Los Alamos, NM 87545

An Affirmative Action/Equal Opportunity Employer

100-7000
This report was prepared under contract with the USG Government by Los Alamos National Laboratory, a Division of the University of California. This report contains neither recommendations nor conclusions of the USG. It is the property of the USG, and is loaned to your agency; it and its contents are not to be distributed outside your agency without the express written consent of the USG. Your agency is responsible for the contents of this report.

A MULTICHANNEL ELECTROSPHERE DATA-AQUISITION SYSTEM¹

John S. Barnes*, Kenneth R. Hogstrom, Roy T. Sallies,
James L. Rosen, and Alfred R. Shultz*

Abstract

A multichannel electrospHERE data-aquisition system, which measured surface currents collected, has been developed for dosimetry purposes off the pilot beam test site at the Clinton P. Anderson Mission Physics Facility (LAMPF) in Los Alamos, New Mexico. This system increases dosimetry data-aquisition rates by a factor equal to the number of dose chambers in use. It is the second in a series developed electrospHERE amplifier compatible off-axis electron beam measurements for plasma-particle interaction studies. Design and construction off the electrospHERE has presented many difficulties, and examples off these difficulties with this system are presented. The effect on the readings due to scattered and background radiation have been measured.

II. Introduction

A multiple ionization chamber array (MICA) dosimetry system has been developed for use on the Bitter-chamber off-axis test site (Clinton P. Anderson Mission Physics Facility (LAMPF)). This system consists off an array off cylindrical ionization chambers whose output charge is collected and measured by a set off computer-controlled electrometers.

In radiobiology there is a need to characterize the radiation fields with extensive dosimetric measurements. This is usually done by collecting measurements with a single ionization chamber throughout an suitable volume in a sequential sampling scheme. This resulting dose can then be converted and plotted as radiation dose distributed in the material and subsequently used for quantitatively planning medical treatments. Therapy with heavy charged particles uses the compatibility off controlling several these parameters such as beam shape (beam selection, convergence), beam spreading (depth) and beam energy (penetration) to optimize radiation dose primarily to the planned treatment volume. The possible combinations off parameter values, coupled with the need for extensive dosimetric measurements (1 to 100 mm resolution throughout volumes and large as 22.55 liters) requires a large number of measurements per field. When the necessary to use computers and human time on a large number results in the LAMPF accelerator, the advantage and ease accessibility off simultaneous multiple measurements are apparent. Multiple-ionization chamber dose aquisition has been done previously,² but not at the low current levels measured here.

*Supported in part by USPHS Grants, No. CA-16927 and CA-14532, National Cancer Institutes, Division of Research Resources and Services, and by other U.S. Department of Energy.

¹University of New Mexico, Cancer Research and Treatment Center, Bio-Medical Physics Section, 9000 University Station, Albuquerque, NM 87131.

III. Design Considerations

The automated dosimetry data-aquisition system for the LAMPF off-axis facility is described below as a single off-axis dose array.³ The present goal was to make this a multichannel system and thus increase the dose-aquisition rates by a factor off ten or more. This has been accomplished by designing and fabricating three separate measuring electrospHERE amplifiers reading the following variables:

- 1) accurate integration off low currents (0.1 to 100 pA);
- 2) computer-controlled zeroing and range switching;
- 3) negligible errors due to small ambient temperature variations ($0.2^{\circ}\pm 5^{\circ}\text{C}$), and electrical warmup times;
- 4) negligible errors from electrical noise in the nearby environment;
- 5) negligible errors on the readings from movement and background radiation.

IV. System Configuration and Operation

The dose-aquisition system has already been discussed through a brief description of the three-dimensional tracking. It includes a three dimensional scanner with computer control for positioning the detectors in the radiation fields.

The detectors consist of 0.05 cm, Al250 thickness plastic,⁴ Spacelab-type ionization chambers, used with carbon-equivalent (CE) neutron gas mixtures. These small chambers can be closely spaced as 2 cm apart without significantly perturbing the radiation fields. Figure 1 shows an array off chambers in their spacer plates.

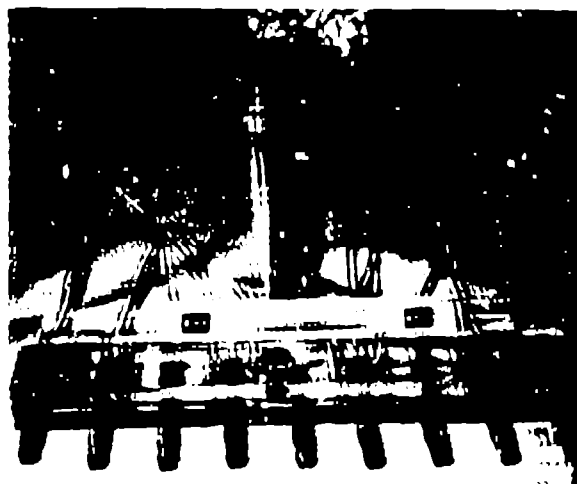


Fig. 1. Array off ionization chambers.

In operation other speaker provides the uncorrected raw data information, and the discriminator in other preprocessor always uses uncorrected raw data whenever one is shown in Figures 2.



Fig. 22. Discriminatory equipment which removes off-discrepancy from vector quantities.

The pickup-app-level current signals generated by the discriminators are measured with four voltmeters and are shown schematically in Figure 11.

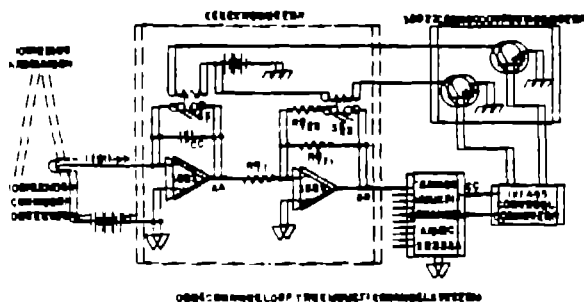


Fig. 11

Hence the voltmeter-app level output signal is a function of discrepancy. The readings are correlated with the integrated readings shown in the dependent counter-integrator monitor, after which the preamplified integrated in the beam lines. SI is a computer-controlled zeroing switch and C is the integrating capacitor. The detailed circuit analysis in the next section will reveal connections on these components as well as on the op-amps.

The CAMAC intelligent-digital converter is an off-the-shelf 12 bit capable of digitizing analog inputs from 0 to 1000 voltages. At 12-bit resolution, 122 kHz ADC results the word to give 0.1% resolution resolution.

Computer controls off-zeroing and range-switching the discriminator via relay modules SI and SC, switched through a 48-channel CAMAC output register module.

Software input specifies the channels, addresses generation, and relay modules associated with each ADC input. The address generation is selective due to individualization within the controlled through the three-dimensional memory.

The software reads the calibrated offset of the gain in the discrimination-and-integrating voltage off each channel and the calibrated capacitance off each discriminator in use from a master data file. This allows the hardware associated with each ADC channel to be changed or to be switched from one channel to another. Any number of channels may be used.

The software controls the data acquisition in the following manner. First the channels are programmed by commanding the master to do so as specified below. The program copies SI to monitor the discriminators, then waits 1/22 second to avoid transients due to switch between and change injected to the discriminator from the switch over. Next the program reads and stores the initial voltages on the ADC channels and the initial counts in the integrator memory channel number units, both off which are monitored by the control computer. Finally the program reads and stores final voltages and actual elapsed time and monitor units and then initializes the discriminators. Then the changes in voltages (ΔV) and elapsed monitor units the program calculates (charge/time)/monitor units for each channel and stores the values together with the discriminator positions as measures of the beam and each position. Change in the current integrated by the discriminators, and the calculated as ΔW. The (charge/time)/monitor units is effectively a normalized dose reading. Then the discriminators are moved to the next designated position and another such measurement is conducted out. In this way the beam can be scanned and characterized along a single line, across a plane, or throughout a volume.

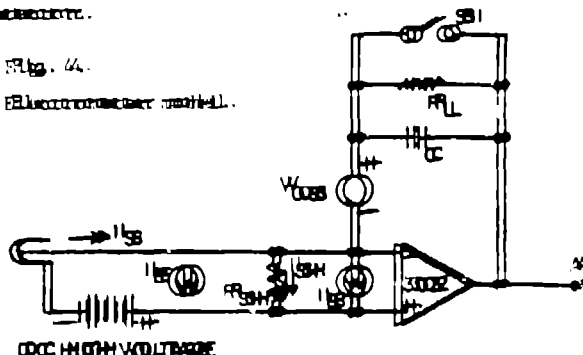
IV. Electronics

Initial width errors analysis

Figures 14 is a simplified analytical model for the discriminator op-amp and its integrating capacitor, zeroing switch, and discriminator from the discriminators.

Fig. 14.

Discriminator model.



In this diagramme different elements are used to model possible sources of error in the following manner. I_{H} represents a path for charge to leak off the integrating capacitor C. This primary component is the insulation resistance off the capacitor C and the sealing sealant S1L. V_{in} is the input offset voltage off the op amp, and I_{B} is the input current offset. I_{SII} represents shunt current excess radiating from several sources. The phenomena involved are: (i) I_{SII} , shunt resistance off the cable and interconnection; (ii) leakage paths between low-current conductors and nearby voltage sources; and (iii) electrostatically-generated currents from static discharges on component surfaces. I_{E} represents unwanted currents generated in the interconnection due to capacitive and piezoelectric effects. Both off these sources for error generation contributes on the insulation off components as well as on the design and on construction techniques. Shilding on these contributions will be discussed after some analysis off the circuit.

Experiments with the insulation thickness in the input stage have set UMEFF to be the leakage off charge to the insulation in a typical 100-second measurement. The minimum expected was 8.55 picoulombs, yielding an average offset current off 0.85 pA. The leakage off the entire system must be less than approximately 1% off this, or error currents $\leq 0.85 \times 10^{-12} \text{ A}$.

Electromagnetic oppamps are available with the compatibility off zeroing input offset voltage. Assuming this limitation on the selection of oppamps eliminates W_{in} from further consideration. Neglecting input current excess reasonably, we can write an expression for the voltage output at point A in Figure 4 as follows:

$$E_A(t) = (-1/C_1) \int_0^t I(t') dt' + V_{\text{in}} \quad (\text{Eq. 1})$$

where $I = I_{\text{SII}}$ and $R = R_{\text{II}}$. Now assuming $C_1 = 100 \text{ pF}$, $\frac{dI}{dt} = 10^{-12} / \text{RC}$, so

$$E_A(t) = (-1/C_1)(1 - e^{-t/\text{RC}}) \int_0^t I(t') dt' + (1 + t/\text{RC}) V_{\text{in}}. \quad (\text{Eq. 2})$$

For most off the applications under consideration it is approximately 100 seconds. For analysis we assume ≈ 1000 seconds. Now assuming the maximum permissible error due to the $R_{\text{II}}C$ leakage to be 1%, Eq. 2 reduces to

$$E_A(t) = -1/C_1 \int_0^t I(t') dt' \quad (\text{Eq. 3})$$

with the constraint ≈ 1000 seconds and $R_{\text{II}}C \approx 10^5$.

Referring now to Figure 11, the voltage output at point B is given by

$$E_B = -(R_H/R_L) E_A = +60/C_1 \int_0^t I(t') dt'. \quad (\text{Eq. 4})$$

where $C = R_H/R_L$ is the load-load voltage gain off the second oppamp stage.

Design and Construction

Several magnitudes off charge collection range are generated by the various bias conditions under which NYCA could be used at UMEFF. These range off values for (C/I) . The analog-to-digital converter is at 12 bit resolution (4096 counts, noiseless output), corresponding to 0 to 100 voltage output signal from the electrometer. Therefore the digitized output is obtained from Eq. 4 as

$$\text{Counts} = 4096 E / V_{\text{DD}} = 4096 C/I \quad (\text{Eq. 5})$$

where C is the charge collected from the detector by the electrometer. In order to make measurements to approximately 1% round-off error (at 12 significant bits), we require a minimum measurement off approximately 822 counts. This minimum measurement would occur at 100% off the bias peak which gives the lowest charge collection rates, or 100% off the 28.5 pC measured earlier, and would be made with the maximum electrometer gain, or noiseless (C/I). For a 100-second resulting this presents a constraint on (C/I) from Eq. 5:

$$C/I \geq 1/55 \quad (\text{Eq. 6})$$

where C is expressed in pC. The lower limit for C/I is determined from the maximum charge-generating rate which is projected to the about 2000 pC in 100 sec, and which must yield counts less than 4096. Again from Eq. 5,

$$C/I \leq 1/200. \quad (\text{Eq. 7})$$

To determine specific values for C and I , we must recall the constraint associated with Eq. 3, i.e., $R_{\text{II}}C \approx 10^5$. This becomes a practical lower limit off about 50 pF for C because practically available resistances in such thin-film resistors are about 10^{15} ohms. Then Eq. 6 yields 0.018. For this reason values off 100 and 2.5 were chosen for C with $C = 50 \text{ pF}$. This gives $C/I = 1/55$, $1/200$, satisfying Eq. 6 and Eq. 7 respectively. To maintain the highest stability a quiescent capacitor is used for C .

This design must consider the input current error sources described in the next. Electromagnetic oppamps with input offset current specified at 10^{-12} A were chosen and then individually selected for lower offset currents down to 10^{-15} A . The shunt resistances off the cable and interconnection were minimized by using low-inductance cables and connectors insulated with Teflon and glass. The connection between the cable insulation and the metal shield minimizes electrostatically-generated current errors. Leakage between low-current conductors and nearby voltage sources was minimized by mounting the electrometer oppamp in a shielded with Teflon insulation pads and by mounting all critical components above the common ground on virgin Teflon substrates. Careful handling off the virgin Teflon substrates avoid piezoelectric effects. Finally, all components and assemblies were thoroughly cleaned with methanol and dried with a stream off dry nitrogen to avoid electrostatically-generated currents.

At the second amplifier stage this signal is sent to both trigger counters itself. An opamp with JFET input has one noninverting bias voltage (negative adjustable also zero), high input impedance, low input current current, and two additional compensation-dependent driftless offsets.

The preamplifier gain is set by using variable-gain preamplifiers with a compensation coefficient of 100 psec/V. After adjusting W_{out} on both opamps, the preamplifier gain is also determined by Housing earth electrocoupler in a compensation loop and placing all three loops in a single well-grounded Housing. Figure 5 shows the connection of an individual electrocoupler, and Figure 6 shows an array of electrocouplers mounted for use.

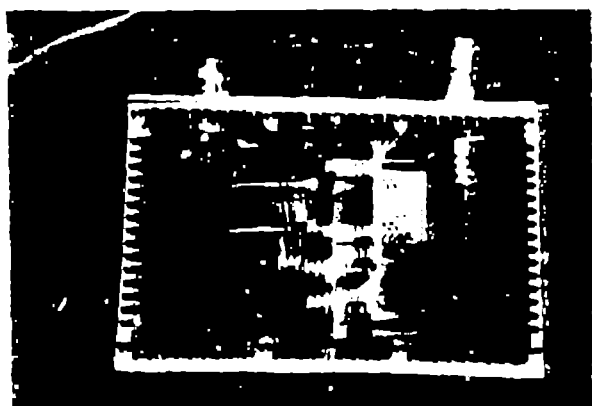


Fig. 5. Electrocoupler connection

The electrocoupler gains are established from electrocoupling ratios. All cables used are shielded cables, including switching-control and power cables. The solid-state power supply that still units receives AC power through an isolation transformer. DC power lines are heavily bypassed to ground at 1225 μ F/VA through earth electrocoupler cases.

V. Performance and Results

Introduction

Unreliability of electrocoupler responses has been measured by supplying a constant current to the input and measuring output voltage versus time. For a well-grounded electrocoupler unreliability due to the nonlinearity of the connection coefficients is 0.99999. Breakdowns were taken from 0 to 1000 seconds and 0 to 100 voltage with an impact of 5pA.

Unreliability

Total current breakdown effects in the absence of nonlinearities were measured by changing the electrocoupler connection to several voltages and measuring output voltage for the output voltage to decay to predetermined amount within no longer present. Measurement times were on the order of 1000 seconds. On a scale of 100 electrocoupler total breakdown currents ranged from 10^{-13} A to a maximum of 7×10^{-15} A, with variation



Fig. 6. Electrocoupler assembly

the leakage connection off 0.856×10^{-14} A.

Reliability Effects

The leakage due to nonlinearities plotted in Figure 7 was measured by two methods.

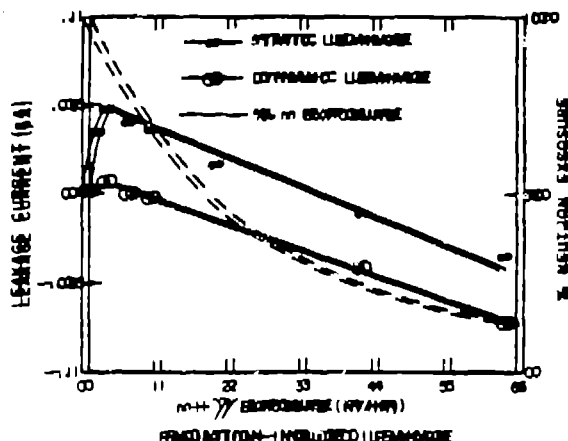


Fig. 7.

In other reliable method the electrocoupler capacitance was respectively changed, impact current removed, and the electrocoupler noise was found to vary significantly with exposure rates from 0 to 60 R/h. A similar dependence was found for the dynamic method which was over the electrocoupler noise while the capacitance for nonradiation changes from a constant-current impact source. However, this method did not show linear leakage currents for exposure rates less than 10 R/h. In both cases the effect of the nonlinear and high exposure levels were too change the capacitance. The leakage currents are less than 0.856×10^{-14} A for exposure rates below

1.184 m in the dynamic mode, exceeding the design configuration. The system is presently used in the gamma and neutron activation experiments rates of only 0.15% /hr. The neutron moderation rate reduction was due to fewer neutrons and was measured with a Bonner sphere.

Results

In Figure 8 we compare these values by MCNA with those taken on a single-channel system.

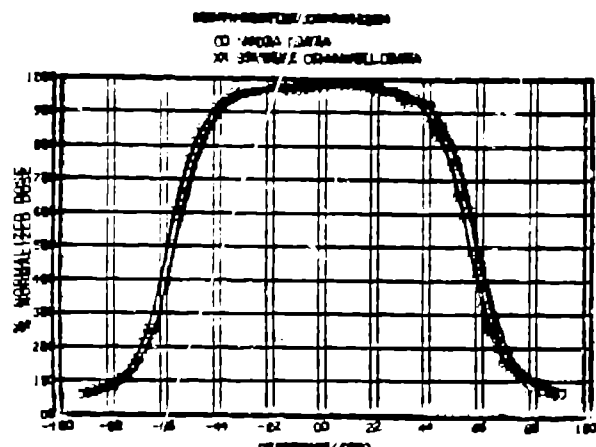


Fig. 8

The two beam profiles agree within 0.5% cover a factor of 100 in dynamic range, illustrating 10% agreement in collective effluent and electromagnetic contributions. This demonstrates the feasibility of using MCNA to replace single-channel dose computation.

VII. Summary and Conclusions

The MCNA system has already increased IANPOF dosimetry dose computation rates by a factor of ten. We have demonstrated 0.5% agreement between the multichannel system and a single-channel system. We have also demonstrated the feasibility of operating the multichannel electromagnetic system under conductive control and taking readings, accurate, independent data from signals not otherwise used. Dose reduction off the critical design and electromagnetic contribution reductions specific sources off sources and techniques for reducing these errors.

Acknowledgments

The authors wish to thank Dr. Charles Kelley for his continuing support and encouragement through our efforts. Scott Wilson provided able technical assistance in constructing the electrometers. Lynn Young helped us with initial evaluation off several different components and design techniques.

Bibliography

11. Johnson, H.E., Randalton, J.A., Thaylur, J.R., "Neutron Dosimeter to Study the Unifority of High Energy X-ray Beams," *American Journal of Roentgenology, Radiation Therapy, and Nuclear Medicine*, **120**, No. 1, pp. 1992-201, Jan., 1974.
12. Rosen, J., Stalith, M., Lorne, R., Kellaway, C., Leslie, B., Hoggarth, K., Somers, J., Helland, J., Kellaway, R., Andrus, H., Thompson, J., and Riddiman, C., "An automated dosimetry data acquisition and analysis system and the IANPOF photon therapy facility," *Medical Physics*, **5**, No. 22, pp. 1220-1223, March/April, 1978.
13. "CENIG-A Multilayer Dosimetry System for Dose Ratiing," ANSI/IEEE Standard SR33-1976 and EURATOM Report EUR-4000/e (1972).
14. Skordis, P.R., Ross, J.E., and Pichler, A., "Conducting Electrolyte dosimetry, Nit, and Polycyano," Paper No. P7/581, Congress Conference on Progress in Nuclear Energy, Session XII, London, Oct. 1971, Vol. II, pp. 1680-1686 (1972).
15. King, J.A.W. and Woodall, J.E., "Evaluation of a High-Resolution Dry-based Scatter for Electromagnetic Applications," *Electronics Engineering*, May, 1970, p. 2316.